MOLECULAR AND CELLULAR BIOLOGY, Aug. 2000, p. 5479–5489 Vol. 20, No. 15
0270-7306/00/$04.00+0
Copyright © 2000, American Society for Microbiology. All Rights Reserved.

Increased Energy Expenditure, Decreased Adiposity, and Tissue-Specific Insulin Sensitivity in Protein-Tyrosine Phosphatase 1B-Deficient Mice

LORI D. KLAMAN,[1] OLIVIER BOSS,[2] ODILE D. PERONI,[2] JASON K. KIM,[3] JENNIFER L. MARTINO,[1] JANICE M. ZABOLOTNY,[2] NADEEM MOGHAL,[1] MARGARET LUBKIN,[4] YOUNG-BUM KIM,[2] ARLENE H. SHARPE,[5] ALAIN STRICKER-KRONGRAD,[4] GERALD I. SHULMAN,[3] BENJAMIN G. NEEL,[1]* AND BARBARA B. KAHN[2]*

Cancer Biology Program, Division of Hematology-Oncology,[1] and Division of Endocrinology,[2] Department of Medicine, Beth Israel Deaconess Medical Center, Harvard Medical School, and Division of Immunology, Brigham and Women's Hospital,[5] Boston, Massachusetts 02215; Howard Hughes Medical Institute, Yale University School of Medicine, New Haven, Connecticut 06536[3]; and Metabolic Diseases Physiology, Millennium Pharmaceuticals, Cambridge, Massachusetts 02139[4]

Received 15 March 2000/Accepted 24 April 2000

Protein-tyrosine phosphatase 1B (PTP-1B) is a major protein-tyrosine phosphatase that has been implicated in the regulation of insulin action, as well as in other signal transduction pathways. To investigate the role of PTP-1B in vivo, we generated homozygotic PTP-1B-null mice by targeted gene disruption. PTP-1B-deficient mice have remarkably low adiposity and are protected from diet-induced obesity. Decreased adiposity is due to a marked reduction in fat cell mass without a decrease in adipocyte number. Leanness in PTP-1B-deficient mice is accompanied by increased basal metabolic rate and total energy expenditure, without marked alteration of uncoupling protein mRNA expression. In addition, insulin-stimulated whole-body glucose disposal is enhanced significantly in PTP-1B-deficient animals, as shown by hyperinsulinemic-euglycemic clamp studies. Remarkably, increased insulin sensitivity in PTP-1B-deficient mice is tissue specific, as insulin-stimulated glucose uptake is elevated in skeletal muscle, whereas adipose tissue is unaffected. Our results identify PTP-1B as a major regulator of energy balance, insulin sensitivity, and body fat stores in vivo.

Obesity and diabetes mellitus represent major public health problems. Type 2 diabetes is a polygenic disease affecting over 100 million people worldwide. The risk of developing type 2 diabetes is increased in populations that lead a sedentary lifestyle and consume a typical western diet, in which more than 50% of the calories are derived from fat (34, 37). A high-fat diet and low energy expenditure predispose to obesity, a condition characterized by increased insulin resistance in insulin-responsive tissues, such as skeletal muscle, liver, and white adipose tissue (9, 42). Body weight also is subject to polygenic regulation (18). Many of the key genes that regulate body mass and glucose homeostasis remain to be identified (27).

Insulin plays a critical role in regulating glucose homeostasis, lipid metabolism, and energy balance. Insulin signaling is initiated by binding of insulin to the insulin receptor (IR), a receptor tyrosine kinase. Insulin binding evokes a cascade of phosphorylation events, beginning with the autophosphorylation of the IR on multiple tyrosyl residues. Autophosphorylation enhances IR kinase activity and triggers downstream signaling events. These include tyrosyl phosphorylation of IR substrate (IRS) proteins (IRS-1 to -4) and other adapter molecules (e.g., Grb2 and Shc), whose combined actions mediate the biological effects of insulin (reviewed in references 24, 43, 54, and 69).

* Corresponding author. Mailing address for Benjamin G. Neel: Cancer Biology Program, Beth Israel Deaconess Medical Center, 330 Brookline Ave., Boston, MA 02215. Phone: (617) 667-2823. Fax: (617) 667-0610. E-mail: bneel@caregroup.harvard.edu. Mailing address for Barbara B. Kahn: Diabetes Unit, Beth Israel Deaconess Medical Center, 99 Brookline Ave., Boston, MA 02215. Phone: (617) 667-5422. Fax: (617) 667-2927.

The extent of tyrosyl phosphorylation on a given protein is controlled by the reciprocal actions of protein-tyrosine kinase and protein-tyrosine phosphatase (PTP) activities. Since insulin stimulation leads to multiple tyrosyl phosphorylation events, enhanced activity of one or more PTPs could lead to insulin resistance. Indeed, increased PTP activity has been reported in several insulin-resistant states, including obesity, and in some models of diabetes (2, 4, 6, 12, 17, 40, 52).

Specific PTPs, including LAR, SHP-2, and PTP-1B, have been implicated in the regulation of normal IR signaling and/or in insulin resistance (1, 2, 3, 6, 13, 39, 44, 45, 46, 51, 53, 62, 68; reviewed in references 19 and 36). Of these, PTP-1B has received significant attention for several reasons. PTP-1B is an abundant enzyme that is expressed in all insulin-responsive tissues, where it is localized predominantly on intracellular membranes by means of a hydrophobic C-terminal targeting sequence (35, 71). Importantly, IR dephosphorylation occurs following receptor endocytosis (26, 30), which could allow the IR to access PTP-1B. In cultured cells, overexpression of PTP-1B inhibits insulin-stimulated phosphorylation of the IR and possibly IRS-1 (45), whereas osmotic loading of anti-PTP-1B antibodies into cells enhances insulin signaling (7). Several studies have examined PTP-1B expression in rodents and humans with insulin resistance and/or diabetes. Many of these show increased expression of PTP-1B in insulin-resistant states, most notably obesity (1, 2, 5, 6), although other work contradicts these conclusions (20, 47, 72). PTP-1B also is implicated in the regulation of other pathways, including the epidermal growth factor receptor (33), cadherin (10), and integrin signaling pathways (8, 48, 49), cell cycle regulation (32, 61), and the response to various cellular stresses (63). Thus,

Downloaded from http://mcb.asm.org/ on June 25, 2019 by guest

the role of PTP-1B in normal physiology and pathologic conditions has remained unclear.

To determine the function of PTP-1B in the whole organism, we generated PTP-1B-null (PTP-1B$^{-/-}$) mice by targeted disruption of the ATG-coding exon (Ex1$^{-/-}$ mutation). While our work was in progress, Elchebly et al. (28) targeted exons 5 and 6 (Ex5/6$^{-/-}$ mutation) and also obtained PTP-1B$^{-/-}$ mice. Their mice exhibited increased insulin sensitivity, as manifested by enhanced phosphorylation of IR and IRS-1 in muscle and liver in response to insulin stimulation. These results are consistent with PTP-1B playing a major role in regulating IR and perhaps IRS-1 tyrosyl phosphorylation. Unexpectedly, they also found that PTP-1B Ex5/6$^{-/-}$ mice failed to gain weight when maintained on a high-fat diet. However, the physiological basis for this finding was unclear. Here, by analyzing body composition in PTP-1B Ex1$^{-/-}$ mice, we find that their low body weight is due largely to a dramatic reduction in body fat content, despite a slightly increased food intake. This resistance to diet-induced obesity is characterized by a marked decrease in adipocyte volume (mass) without alteration in adipocyte number. Furthermore, we show that PTP-1B-deficient mice are hypermetabolic, with increases in both basal metabolic rate and total energy expenditure. Our PTP-1B Ex1$^{-/-}$ mice also exhibit increased insulin sensitivity and enhanced glucose tolerance. In hyperinsulinemic-euglycemic clamp analyses, we find that the elevated whole-body insulin sensitivity in PTP-1B-deficient mice results mainly from increased glucose utilization in skeletal muscle, whereas that in adipose tissue is unchanged. Our results indicate that PTP-1B is a critical regulator of energy expenditure and body fat stores, as well as a tissue-specific regulator of insulin sensitivity.

MATERIALS AND METHODS

Generation of PTP-1B-deficient mice. P1 clones were obtained from a mouse ES-129/SvJ genomic library (Genome Systems, St. Louis, Mo.) using PTP-1B primers (5′-CAT CCA GAA CAT GCA GAA GCC GCT-3′ and 5′-TTC CCA GCC TTG TCG ATC TC-3′). An 11-kb *Hin*dIII fragment containing the ATG-coding exon was subcloned into pBlueScript (Stratagene, La Jolla, Calif.). A targeting construct, designed to replace the ATG-coding region (located within exon 1) and 2.3 kb of flanking sequence, was generated by ligating a 1.2-kb *Sac*II(R1)-*Xho*I fragment (left arm) and a 4.8-kb *Bam*HI-(R1)*Sal*I fragment (right arm) of the PTP-1B gene into the *Sac*II and *Nhe*I/*Sal*I sites of the vector pSABGal-pgkneolox2PGKDTA (obtained from A. Immamoto, University of Chicago, Chicago, Ill.), respectively. The targeting vector (25 μg) was linearized at the unique *Not*I site and electroporated (25 μF and 400 V) into 10^7 J1 embryonal stem (ES) cells (obtained from R. Jaenisch, Massachusetts Institute of Technology, Cambridge). G418 (400 μg/ml)-resistant colonies were screened for homologous recombination events using PCR. The forward and reverse primers were 5′-GTG CTC TTA ACT GCT GAG CC-3′ and 5′-GCG AGC TGT GGA AAA AAA AG-3′, respectively. PCR-positive heterozygotic ES clones were verified by Southern blot analysis. Briefly, *Hin*dIII-digested DNA was hybridized to probe A, corresponding to a 400-bp region upstream of the area of homologous recombination, and subsequently to probe B (carrying a neomycin resistance cassette) *neo* to ensure that only a single integration event occurred. Chimeric mice were generated by injection of three independent PTP-1B$^{+/-}$ ES clones into C57BL6/J blastocysts. Male chimeras were mated with C57BL6/J or 129/SvJ females to produce PTP-1B$^{+/-}$ offspring, which were interbred to produce PTP-1B$^{-/-}$ mice. Offspring were genotyped by PCR and Southern blot analysis. All experiments herein were performed using mice on the hybrid 129/SvJ × C57BL6/J background. Similar results were obtained with all three clones.

Antibody production. To produce antibodies reactive against murine PTP-1B, full-length murine PTP-1B cDNA was subcloned in frame into the bacterial expression vector pGEX 3X (Pharmacia). Glutathione *S*-transferase (GST) fusion protein was produced and used to immunize New Zealand White rabbits, and affinity-purified antibodies were prepared by passing antisera sequentially over GST and GST–PTP-1B bound to Affi-Gel 15 (Bio-Rad) as described previously (35).

Northern and immunoblotting. RNA isolation and Northern blotting were performed as described elsewhere (15). Blots were hybridized to ^{32}P-labeled PTP-1B (full length), UCP (uncoupling protein [14]), β-actin (Clontech, Palo Alto, Calif.), or glyceraldehyde-3-phosphate dehydrogenase (GAPDH) cDNA. Tissue homogenates were prepared using Nonidet P-40 buffer, analyzed by sodium dodecyl sulfate-polyacrylamide gel electrophoresis, and transferred to Immobilon-P membrane (Millipore, Bedford, Mass.). Immunoblots were probed with affinity-purified mouse PTP-1B rabbit polyclonal and detected by enhanced chemiluminescence.

Animal care and diet treatment. Animal studies were conducted according to federal guidelines (53a). Mice were housed at 24°C on a fixed 12-h light/dark cycle. Animals had free access to either a chow (product no. 5020; Purina, St. Louis, Mo.) or high-fat diet (product no. 93075; Harlan-Teklad, Madison, Wis.). The chow diet consisted of 22% fat, 57% carbohydrate, and 0.7% sucrose (calorie content), whereas the high-fat diet was 54% fat, 25% carbohydrate, and 7.6% sucrose. Both diets contained 21% of the calories as protein. The high-fat diet was supplemented with Harlan-Teklad vitamin (product no. 40060) and mineral (product no. 170915) mixes. The physiological fuel values were 3.8 and 4.8 kcal g^{-1} for the low- and high-fat diets, respectively. Age- and sex-matched littermates were used for each experiment. Food intake and body weight were measured weekly.

Metabolic measurements. Randomly fed or fasted (12 h) mice were analyzed as indicated. Blood glucose was assayed with a glucometer (Lifescan, Milpitas, Calif.). Serum insulin was determined by enzyme-linked immunosorbent assay, using mouse insulin as a standard (Crystal Chem Inc., Chicago, Ill.). Free fatty acid (FFA) values were measured by an enzymatic colorimetric method (Wako, Neuss, Germany). Serum leptin was assayed by radioimmunoassay (Linco, St. Charles, Mo.). Glucose tolerance tests (GTTs) were performed on fasted (12 h) mice. Animals were injected intraperitoneally with D-glucose (20% solution; 2 g/kg of body weight), and blood glucose values were determined at 0, 15, 30, 60, and 120 min postinjection. Insulin tolerance tests (ITT) were performed on fasted (6 h) animals. Blood glucose values were measured immediately before and at 15, 30, 60, and 120 min after intraperitoneal injection of human crystalline insulin (0.75 U/kg of body weight; Eli Lilly Corp., Indianapolis, Ind.).

Hyperinsulinemic-euglycemic clamp study. A 120-min hyperinsulinemic-euglycemic clamp was performed in conscious, fasted (16 h) mice as described elsewhere (56). Human insulin was infused at a constant rate of 2.5 mU^{-1} kg min^{-1}, and blood samples (20 μl) were collected at 20-min intervals to analyze plasma glucose (Glucose Analyzer II; Beckman Instruments, Inc.). Twenty percent glucose was infused to maintain plasma glucose at basal concentrations during insulin infusion. A [3-^{3}H]glucose tracer (10-μCi bolus, followed by 0.1 μCi min^{-1}; New England Nuclear, Boston, Mass.) was infused throughout the clamp to estimate insulin-stimulated whole-body glucose flux. Insulin-stimulated glucose transport in individual tissues was estimated by administration of a bolus (10 μCi) of 2-deoxy-D-[1-^{14}C]glucose (2-[^{14}C]DG; New England Nuclear) 45 min before the end of the clamp. Blood samples (20 μl) also were obtained during the last 40 min of the clamp to measure plasma glucose specific activity. At 120 min, animals were sacrificed and gastrocnemius, epididymal adipose tissue, and liver were immediately frozen in liquid nitrogen. Rates of whole-body glucose uptake and hepatic glucose production were calculated as described elsewhere (56). Plasma samples were treated as previously (56) and counted to determine [3-^{3}H]glucose and 2-[^{14}C]DG specific activity. Glucose transport activity in individual tissues was calculated from plasma 2-[^{14}C]DG using a double exponential curve and tissue 2-DG-6-P content as previously described (73). Fat pad mass, which was consistently threefold lower for PTP-1B$^{-/-}$ mice (0.274 ± 0.030 g for PTP-1B$^{-/-}$ versus 0.954 ± 0.160 for PTP-1B$^{+/+}$ [wild type {WT}], P = 0.002), was divided by the number of adipocytes recovered per depot (~10^6 cells for both genotypes) to determine number of adipocytes per gram of white adipose tissue. This number was multiplied by the glucose disposal rate (nanomoles per minute) per gram of white adipose tissue to calculate glucose disposal rate per adipocyte. Whole-body glycolysis rate was calculated from the linear increase in plasma ^3H_2O between 80 and 120 min. Rates of whole-body glycogen and lipid synthesis were estimated by subtracting the rate of glycolysis from that of glucose uptake.

Adipose cell glucose uptake. Adipocytes were isolated from epididymal fat pads by collagenase (1 mg ml^{-1}) digestion as described elsewhere (67). A fraction of isolated adipocytes was removed to determine average cell number and cell volume (micrograms of lipid per cell) (22). For glucose transport, cells were incubated at 37°C with constant agitation in a 10% (by volume) suspension of Krebs-Ringer HEPES (20 mM) buffer (pH 7.4)–2.5% bovine serum albumin (fraction V)–200 nM adenosine for 30 min without (basal) or with insulin. Glucose uptake was then assayed by a further 30-min incubation with 3 μM [U-^{14}C]glucose (286 mCi mmol^{-1}; Amersham). The reaction was terminated by a 30-s spin over dinonyl phthalate oil, and the upper phase containing the cell layer was counted in a scintillation counter. Under these conditions, glucose uptake directly reflects glucose transport (67).

Body composition. Carcasses (with the food content of their gastrointestinal tracts removed) were weighed, dried in a 60°C oven, reweighed to determine water content, and hydrolyzed in ethanolic potassium hydroxide (60). Body lipid (triglyceride) content was determined by enzymatic measurement of glycerol (product no. 337-40A; Sigma).

Energy expenditure. In vivo indirect open circuit calorimetry was performed in metabolic chambers attached to a feeding monitor system. Constant airflow (0.75 liters/min) was drawn through the chamber and monitored by a mass-sensitive flowmeter. To calculate oxygen consumption (VO_2), carbon dioxide production (VCO_2), and respiratory quotient (RQ; ratio of VCO_2 to VO_2), gas concentrations were monitored at the inlet and outlet of the sealed chambers. Basal (light

Downloaded from http://mcb.asm.org/ on June 25, 2019 by guest

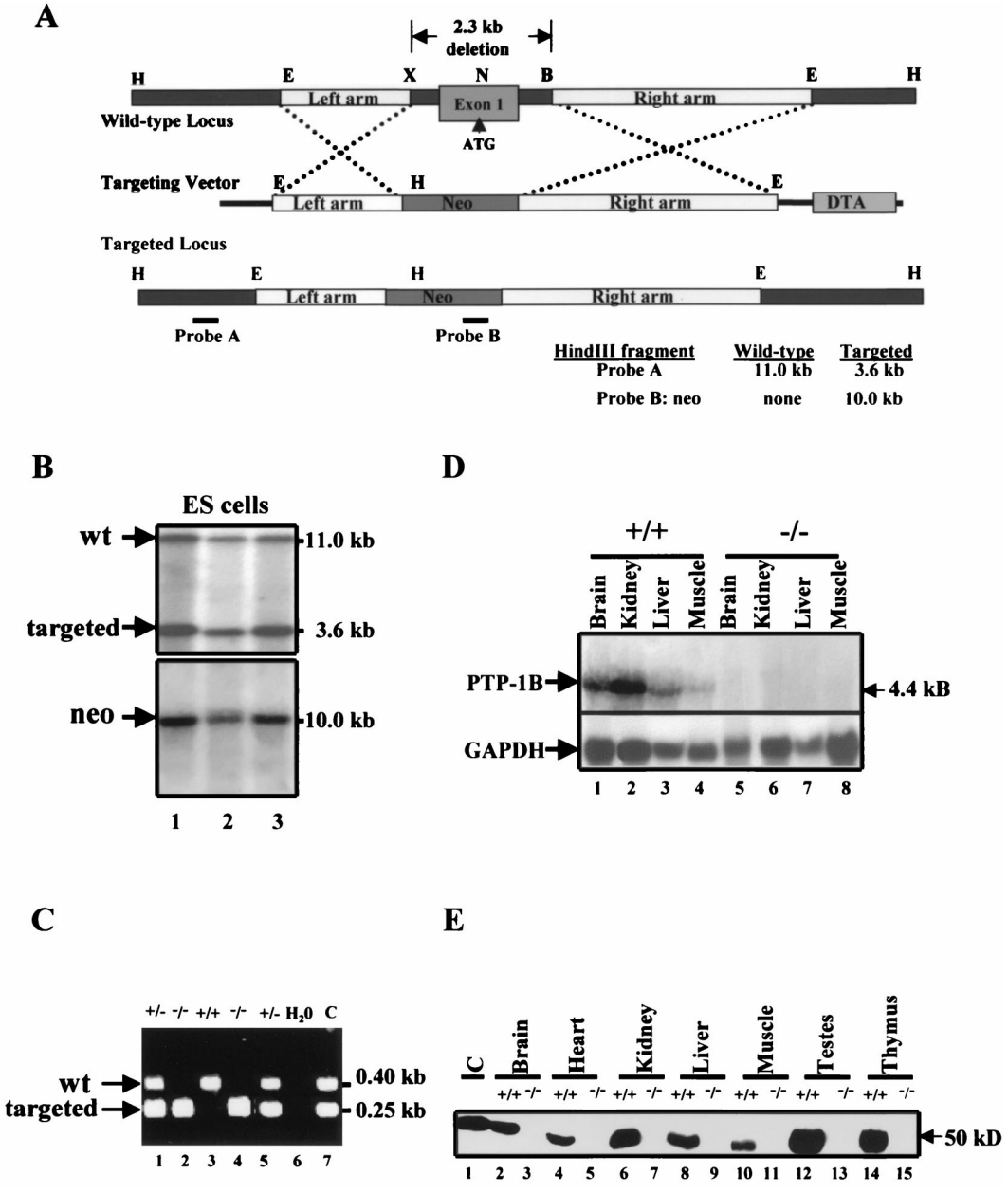

FIG. 1. Gene targeting of the PTP-1B locus. (A) Restriction map of PTP-1B genomic locus (top), targeting vector (middle), and targeted locus after homologous recombination (bottom). B, *Bam*HI; E, *Eco*RI; H, *Hin*dIII; N, *Nco*I; X, *Xho*I. Probes A and B (as indicated; see Materials and Methods) were used to screen for homologous recombinants by Southern blotting. (B) Southern blot analysis of PCR-positive ES clones. ES cell DNA was digested with *Hin*dIII and hybridized to a 0.4-kb external genomic fragment (probe A). An 11.0-kb and a 3.6-kb band are indicative of the WT and recombinant alleles, respectively. The blot was stripped and hybridized to *neo* (probe B) to detect a 10.0-kb band. (C) PCR genotyping of tail DNA distinguishing PTP-1B$^{+/-}$ and PTP-1B$^{-/-}$ from WT mice. H_2O and C are negative and positive controls, respectively. (D) Northern blot analysis of total RNA of tissues from PTP-1B$^{-/-}$ or WT mice hybridized to full-length PTP-1B cDNA. GAPDH hybridization is shown as a loading control. (E) Immunoblot analysis of tissue extracts from PTP-1B$^{-/-}$ or WT mice. Each lane represents a sample from one animal and is representative of three independent experiments. Lane C, control (NIH 3T3 fibroblast extract).

cycle/fasted animals) and total metabolic rate (continuous-24 h/freely fed animals) were calculated from O_2 consumption and CO_2 production. Feeding episodes were monitored with precision balances, and were continuously recorded to calculate food intake.

Statistical analyses. Data are expressed as means ± standard error of the mean (SEM) and were calculated using InStat (GraphPad Software, San Diego, Calif.). The significance of the differences in mean values between groups was evaluated by Student's two-tailed unpaired *t* test. GTTs, ITTs, and body weight curves were analyzed by one-way analysis of variance with a Bonferroni multiple comparison posttest. Curve fitting was performed with the sigmoid model using Origin 3.5 (Microcal Software, Inc.). Differences were considered significant at $P < 0.05$.

RESULTS

Generation of PTP-1B-deficient mice. We constructed a targeting vector that replaces 2.3 kb of PTP-1B genomic sequence, including the ATG-coding exon, with a *neo* cassette (Fig. 1A). The targeting vector was electroporated into J1 ES cells, and G418-resistant clones were screened by PCR to detect homologous recombinants. Of 197 clones analyzed, 12 exhibited the desired mutation and a single vector integration site, as confirmed by Southern blotting with PTP-1B- and *neo*-

Downloaded from http://mcb.asm.org/ on June 25, 2019 by guest

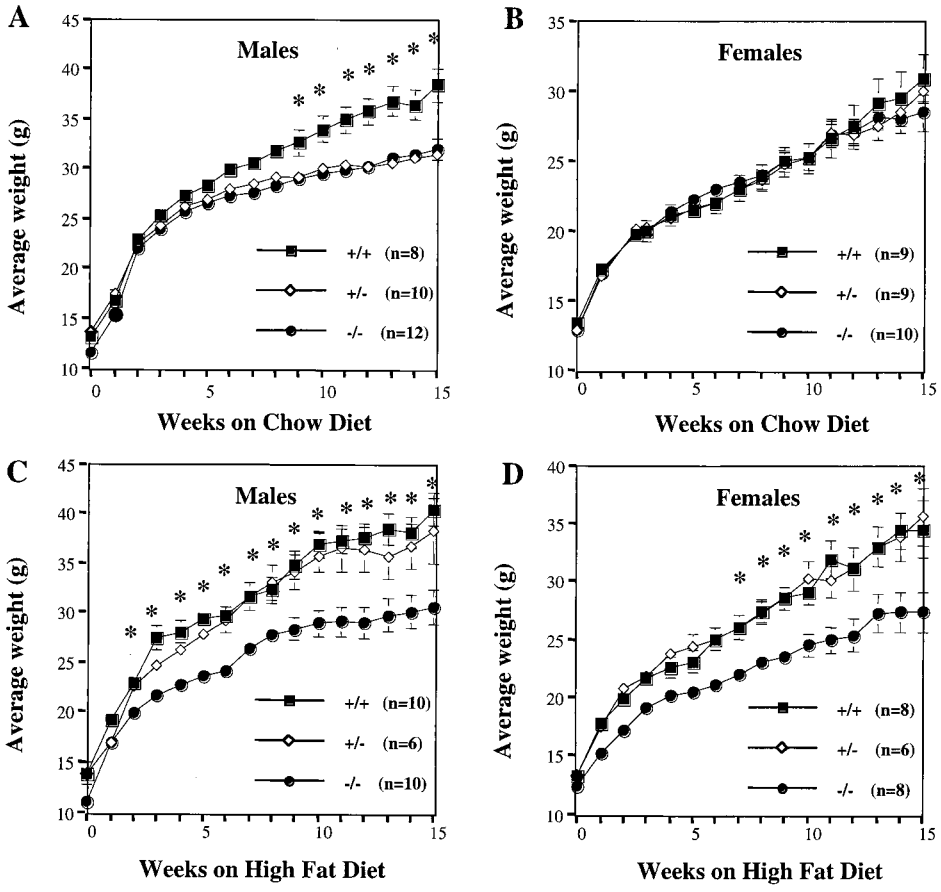

FIG. 2. Body weights of WT, PTP-1B$^{+/-}$, and PTP-1B$^{-/-}$ mice. (A and B) Male (A) and female (B) body weight curves of age-matched WT (+/+), PTP-1B$^{+/-}$ (+/−), and PTP-1B$^{-/-}$ (−/−) mice fed a chow diet for 15 weeks postweaning. (C and D) Male (C) and female (D) body weight curves of age-matched WT, PTP-1B$^{+/-}$, and PTP-1B$^{-/-}$ mice fed a high-fat diet for 15 weeks postweaning. The number of mice in each group is indicated. Values depict mean ± SEM. An asterisk indicates differences between PTP-1B$^{-/-}$ and WT groups where $P < 0.05$.

specific probes, respectively (Fig. 1B). Three independent clones were injected into C57BL6/J blastocysts to generate chimeric mice; all three clones contributed to the germ line of the chimeras. These chimeras were used to establish three independent lines of PTP-1B-deficient mice. Mice from all three lines displayed the same phenotype, which is described in detail below.

Heterozygotic mice from each of these lines were intercrossed, and their offspring were genotyped by PCR and Southern blotting (Fig. 1C and data not shown). All three genotypes (PTP-1B$^{+/+}$, PTP-1B$^{+/-}$, and PTP-1B$^{-/-}$) were obtained at the expected 1:2:1 Mendelian frequency (106:215:95, $P > 0.5$). Absence of PTP-1B expression was verified by Northern analysis (Fig. 1D) and by immunoblotting of tissue extracts (Fig. 1E). Heterozygotic (PTP-1B$^{+/-}$) and homozygotic (PTP-1B$^{-/-}$) mice were viable and fertile in the C57BL6/J × 129/SvJ hybrid background, as well as when the mutation was transferred onto pure 129/SvJ and C57BL6/J backgrounds (see Materials and Methods). Such mice could be maintained for at least 14 months without apparent gross or histopathological abnormalities.

PTP-1B-deficient mice are lean and protected from diet-induced obesity. When PTP-1B$^{-/-}$ males were weaned onto a chow diet, they gained less weight than WT littermates over a 15-week period (Fig. 2A). This difference first became significant 9 weeks postweaning. By 15 weeks, male PTP-1B$^{-/-}$ mice weighed 16% less than controls ($P = 0.001$). Heterozygotic PTP-1B$^{+/-}$ males, whose expression of PTP-1B protein was 50% that of WT mice (data not shown), also gained significantly less weight than WT male mice on this diet (Fig. 2A). Interestingly, no weight differences were observed in females on the chow diet, suggesting that the effect of PTP-1B deficiency may be gender specific (Fig. 2B).

Since PTP-1B-deficient males gained less weight on a chow diet than WT controls, we asked whether these mice also were protected from the increased adiposity normally induced by high-fat feeding. Remarkably, when fed a 55% fat (caloric content) diet for 4 months, male PTP-1B$^{-/-}$ mice remained lean (Fig. 2C), with peak weights comparable to those of PTP-1B$^{-/-}$ males on a chow diet. Unlike mice maintained on the chow diet, however, heterozygotic PTP-1B$^{+/-}$ males fed the high-fat diet gained similar amounts of weight as WT male littermates. These data raise the possibility that dietary fat content may influence the sensitivity of mice to alterations in their PTP-1B levels (see Discussion). Female PTP-1B$^{-/-}$ mice fed the high-fat diet also exhibited significantly lower weight gain than WT female controls. These findings indicate that PTP-1B contributes to body weight regulation in mice (Fig. 2D).

PTP-1B$^{-/-}$ mice have low body fat stores. We analyzed the cause of the decreased body mass in PTP-1B$^{-/-}$ males in detail. Epididymal, inguinal, subcutaneous, and interscapular

Downloaded from http://mcb.asm.org/ on June 25, 2019 by guest

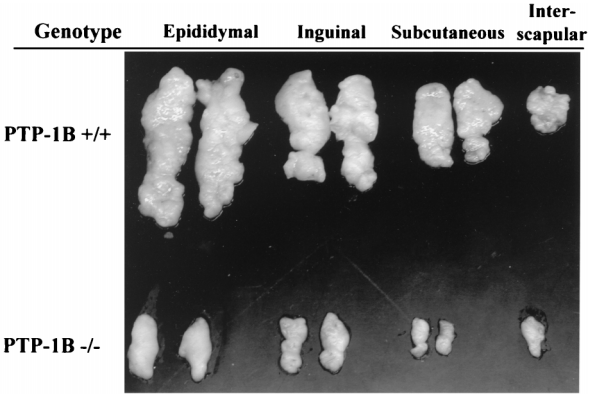

FIG. 3. Reduced white fat pad size in PTP-1B$^{-/-}$ mice. Epididymal, inguinal, subcutaneous, and interscapular white fat pads were dissected from PTP-1B$^{-/-}$ and WT mice, and those from one representative animal of each genotype are displayed.

fat pad weights were reduced threefold ($P < 0.03$) in high-fat-fed PTP-1B$^{-/-}$ mice (Fig. 3 and Table 1). White fat pad mass was reduced similarly in male PTP-1B$^{-/-}$ mice on the chow diet (data not shown; $P < 0.03$). This difference was marked by a 2.6-fold decrease in average cell volume (0.203 ± 0.024 μg of lipid cell^{-1} for PTP-1B$^{-/-}$ versus 0.525 ± 0.076 for PTP-1B$^{+/+}$; $P < 0.03$). Conversely, adipocyte cell number was unaffected by the PTP-1B genotype (~10^6 adipocytes recovered per epididymal fat pad; $P = 0.13$). Brown adipose tissue (BAT) mass also was unaffected in PTP-1B$^{-/-}$ mice (Table 1). These data suggest that at least part of the difference in body weight in male PTP-1B$^{-/-}$ mice is due to decreased lipid content in their adipocytes.

To address this possibility directly, we carried out body composition analyses on male mice maintained on the high-fat diet (Table 2). Compared to WT males, PTP-1B$^{-/-}$ and heterozygotic PTP-1B$^{+/-}$ males weighed on average 38% ($P = 0.007$) and 10% less ($P = 0.4$), respectively. Notably, carcass lipid (triglyceride) content and lipid, expressed as percentages of total body weight, were 72 and 55% lower ($P < 0.002$), respectively, in PTP-1B$^{-/-}$ males compared to WT controls. Differences in fat and, to a lesser extent, water content accounted for most of the decrease in body mass in PTP-1B$^{-/-}$ male mice. There was a small (~7%) decrease in fat-free dry mass when expressed as a percentage of total body weight (Table 2) and in crown-rump length in PTP-1B$^{-/-}$ mice compared to WT mice. Notably, however, weights of organs (e.g., heart, kidney, and testes) and skeletal muscles (e.g., soleus and tibialis anterior) were similar (data not shown). Our results clearly demonstrate that absence of PTP-1B expression has dramatic effects on body composition in mice.

Lower weight in PTP-1B$^{-/-}$ mice is due to increased energy expenditure. The decreased adiposity and resistance to diet-induced obesity could result from decreased food intake, fat malabsorption, and/or increased energy expenditure. Food intake (normalized to body mass) tended to be higher in PTP-1B$^{-/-}$ mice than in WT mice ($P = 0.052$). PTP-1B-deficient mice did not have detectable lipid in their stools, nor was their stool mass different from that for WT mice (data not shown). These data strongly suggested that energy dissipation was increased as a consequence of PTP-1B deficiency.

We determined the basal metabolic rate (BMR) and total daily energy expenditure (EE) in high-fat-fed male mice by measuring VO_2 and VCO_2. BMR (standardized for body weight) was increased by 22% in PTP-1B$^{-/-}$ mice ($P = 0.002$), whereas the RQs (RQ = VCO_2/VO_2) of fasted WT and mutant mice were the same (Fig. 4A). Thus, both genotypes use similar proportions of fat and carbohydrate as fuel substrates under basal conditions, but PTP-1B$^{-/-}$ mice dissipate more energy than WT mice. Total daily EE also was increased significantly in PTP-1B$^{-/-}$ mice (+24%; $P < 0.0001$) and was accompanied by an increase in RQ ($P = 0.03$) (Fig. 4B). Thus, under active conditions, PTP-1B$^{-/-}$ mice use a higher ratio of carbohydrate to fat than do WT mice. Consistent with their elevated metabolic rates, PTP-1B$^{-/-}$ mice displayed a significant increase in core body temperature (38.7 ± 0.13°C for PTP-1B$^{-/-}$ versus 38.2 ± 0.10 for PTP-1B$^{+/+}$; $P = 0.006$). Notably, serum T4 levels were normal (not shown). The similar percentage difference in BMR and EE between WT and PTP-1B$^{-/-}$ mice suggests that they have similar levels of locomotor activity, although direct measurements of activity were not obtained. Thus, the decreased weight of PTP-1B$^{-/-}$ mice apparently results from lowered metabolic efficiency, which causes them to dissipate excess energy as heat, rather than storing it as fat.

Increased EE in PTP-1B-deficient mice is not due to alterations in leptin or UCP mRNA levels. The observation that BMR and total EE were increased to a similar extent in PTP-1B-deficient mice suggests an increase in adaptive thermogenesis, the process by which an organism dissipates excess energy as heat (41, 50). Although there are many potential mechanisms for increased energy dissipation (see Discussion), in rodents, adaptive thermogenesis is often mediated by enhanced uncoupling of electron transport from oxidative phosphorylation (57, 59, 65). Uncoupling can be promoted by increased expression of UCPs in brown fat and/or skeletal muscle, the major thermogenic tissues in rodents (14, 16, 31, 58). However, levels of expression of RNAs of the known UCPs (UCP1, -2, and -3) in BAT and skeletal muscle were similar in high-fat-fed PTP-1B$^{-/-}$ and WT mice (Fig. 5) (see Discussion). Although UCP1 is found at highest levels in brown fat, some white fat depots also express trace amounts of this protein under normal conditions (21), and UCP1 mRNA expression in white fat is induced in response to thermogenic stimuli, such as cold and hypercaloric diets (38). Nevertheless, there was no difference in UCP1 mRNA expression in white fat depots (epididymal and inguinal) between PTP-1B$^{-/-}$ and WT mice (data not shown). Thus, increased UCP1 expression

TABLE 1. High-fat-fed PTP-1B$^{-/-}$ mice have reduced fat pad mass[a]

Genotype (n = 5)	Mean fat pad mass ± SEM				
	Epididymal	Inguinal	Subcutaneous	Interscapular	BAT
WT	1.968 ± 0.183[a]	1.050 ± 0.153[a]	0.418 ± 0.104[a]	0.278 ± 0.020[a]	0.081 ± 0.014[a]
PTP-1B$^{-/-}$	0.666 ± 0.118[b]	0.318 ± 0.097[b]	0.108 ± 0.048[b]	0.071 ± 0.034[b]	0.080 ± 0.007[a]

[a] Male PTP-1B$^{-/-}$ and WT mice were fed a high fat-diet ad libitum for 16 weeks. Body weight and food intake were measured weekly. Mice were killed at 20 weeks of age, and the mass of individual fat pad depots was determined. Values in the same column not sharing a superscript letter are significantly different ($P < 0.05$).

Downloaded from http://mcb.asm.org/ on June 25, 2019 by guest

TABLE 2. High-fat-fed PTP-1B$^{-/-}$ mice have reduced body fat stores[a]

Genotype (*n*)	Mean carcass composition ± SEM					
	BW (g)	Water (g)	Lipid		Fat-free dry mass	
			g	% BW	g	% BW
WT (7)	40.57 ± 3.81[a]	18.84 ± 1.12[a]	8.43 ± 1.24[a]	19.96 ± 1.40[a]	13.30 ± 1.54[a]	32.44 ± 0.94[a]
PTP-1B$^{+/-}$ (5)	36.60 ± 3.14[a]	18.24 ± 0.98[a,b]	6.82 ± 1.38[a]	17.72 ± 2.24[a]	11.54 ± 0.93[a]	31.74 ± 1.21[a,b]
PTP-1B$^{-/-}$ (9)	25.33 ± 1.44[b]	15.38 ± 0.81[b]	2.40 ± 0.41[b]	8.97 ± 1.34[b]	7.56 ± 0.39[b]	29.98 ± 0.37[b]

[a] Male PTP-1B$^{-/-}$, PTP-1B$^{+/-}$, and WT mice were fed a high-fat diet ad libitum for 16 weeks. Body weight (BW) and food intake were measured weekly. Mice were killed at 20 weeks of age, and total carcass fat (triglycerides), fat-free dry mass, and water content were determined. Values in the same column not sharing a superscript letter are significantly different ($P < 0.05$).

is unlikely to account for the substantially increased EE in PTP-1B-deficient mice.

Leptin, a cytokine produced by adipocytes (74), typically reflects body fat levels and has major effects on body mass regulation. The main action of leptin is exerted in the hypothalamus, where it causes decreased appetite, but leptin also may increase EE (11, 29). Consistent with their lower body fat stores, chow-fed PTP-1B$^{-/-}$ males had serum leptin levels that were 64% lower ($P = 0.02$) than those of WT controls. Moreover, high-fat feeding induced a profound increase in circulating leptin concentration in WT mice, whereas serum leptin in PTP-1B$^{-/-}$ animals remained low (Table 3). Likewise, leptin mRNA, measured in white adipose tissue, was reduced by 60% ($P = 0.002$) in PTP-1B$^{-/-}$ mice (data not shown). Thus, rather than contributing causally to their decreased body mass by increasing EE, leptin levels apparently reflect the decreased adiposity of PTP-1B-deficient animals. Finally, we evaluated serum FFA levels in WT and PTP-1B-deficient mice (Table 3). Despite their marked decrease in fat stores, PTP-1B$^{-/-}$ mice had similar levels of serum FFA in both the fed and fasted states compared to WT mice.

Altered glucose homeostasis and enhanced insulin sensitivity in PTP-1B$^{-/-}$ mice. PTP-1B has been implicated in the regulation of insulin action (see the introduction). We therefore compared glucose homeostasis in WT and PTP-1B-deficient mice. Fasting and fed blood glucose levels of chow-fed PTP-1B$^{-/-}$ male mice were significantly lower than those of WT controls (Table 3). Consistent with these data, male PTP-1B$^{-/-}$ mice also had a considerably enhanced ability to clear glucose from the peripheral circulation during intraperitoneal GTTs (Fig. 6A). In contrast, blood glucose levels ($P = 0.21$) (data not shown) and GTTs (Fig. 6B) were unaltered in chow-fed PTP-1B$^{-/-}$ female mice. These gender differences in glucose tolerance correlate with the gender differences in body weight (Fig. 2) on the chow diet.

To determine whether increased insulin sensitivity accounts for the improved glucose tolerance, we measured serum insulin levels and insulin tolerance in vivo. In the chow-fed state, circulating insulin was decreased by 36 and 57%, respectively, in PTP-1B$^{+/-}$ and PTP-1B$^{-/-}$ males (Table 3). Likewise, PTP-1B$^{-/-}$ male mice showed a significantly greater decrease in blood glucose during ITTs (Fig. 6C). Thus, insulin sensitivity is enhanced in PTP-1B$^{-/-}$ male mice. Notably, ITTs of female WT and PTP-1B$^{-/-}$ mice on the chow diet were similar (Fig. 6D).

On the high-fat diet, fed and fasted glucose and insulin levels remained low in male PTP-1B$^{-/-}$ mice ($P < 0.03$) (Table 3). Even on the high-fat diet, PTP-1B$^{-/-}$ mice could dispose of a glucose load with similar kinetics to that of chow-fed PTP-1B$^{-/-}$ mice (Fig. 6E). Moreover, insulin sensitivity, measured more directly with ITTs, remained elevated in male PTP-1B$^{-/-}$ mice on the high-fat diet (Fig. 6F).

To gain detailed insight into glucose utilization in PTP-1B$^{-/-}$ males, we performed hyperinsulinemic-euglycemic clamp studies. The glucose infusion rate necessary to maintain euglycemia (110 mg dl^{-1}) in the presence of a constant infusion of insulin (2.5 mU kg^{-1} min^{-1}) was nearly twofold higher in PTP-1B$^{-/-}$ mice than in the WT controls (443 ± 16.1 μmol kg^{-1} min^{-1} for PTP-1B$^{-/-}$ versus 237 ± 9.88 for PTP-1B$^{+/+}$; $P < 0.0001$). Accordingly, the insulin-stimulated whole-body glucose disposal rate was increased by 80% in PTP-1B$^{-/-}$ mice ($P < 0.0001$) (Fig. 7A). This was accompanied by significant increases in whole-body glycolysis ($P = 0.01$) (Fig. 7B) and in nonoxidative glucose metabolism ($P = 0.0003$) (Fig. 7C).

To identify the tissue(s) responsible for this increase, we quantified glucose uptake into insulin-responsive tissues. Glucose uptake into skeletal muscle was 75% higher in PTP-1B$^{-/-}$ mice than in controls ($P = 0.006$) (Fig. 7D), and there appeared to be a trend toward enhanced suppression of endogenous glucose production in PTP-1B$^{-/-}$ mice (16 ± 4.11 μmol g^{-1} min^{-1} for PTP-1B$^{-/-}$ versus 25.11 ± 3.33 for PTP-1B$^{+/+}$; $P = 0.13$). To calculate glucose uptake into fat, we standardized for the number of cells per fat pad (see Materials and Methods). Glucose utilization in white adipose tissue, in contrast to that in skeletal muscle, was not significantly different between PTP-1B$^{-/-}$ and WT mice ($P = 0.3$) (Fig. 7E). To confirm these findings, we measured insulin-stimulated glucose transport in isolated adipocytes from PTP-1B$^{-/-}$ and WT con-

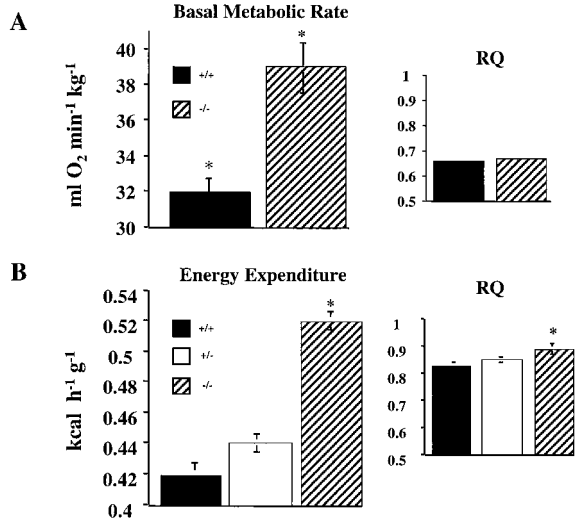

FIG. 4. BMR, total daily EE, and RQ of WT, PTP-1B$^{+/-}$, and PTP-1B$^{-/-}$ mice. BMR and RQ (A) and total daily EE and RQ (B) were measured by indirect calorimetry in male mice fed a high-fat diet for 16 weeks. Results are means ± SEM for five to eight animals per genotype (*, $P < 0.05$).

Downloaded from http://mcb.asm.org/ on June 25, 2019 by guest

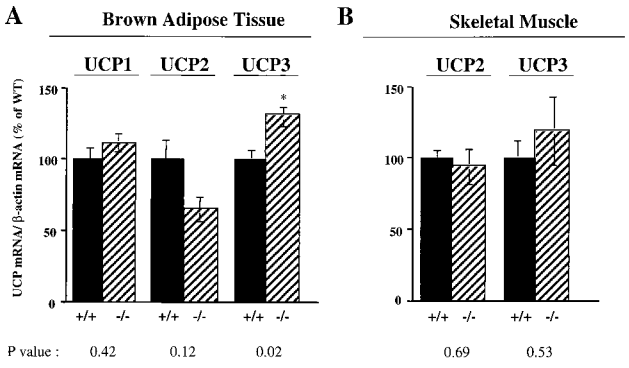

FIG. 5. UCP expression in BAT and skeletal muscle of high-fat-fed PTP-1B$^{-/-}$ and WT mice, determined by Northern blot analysis of total RNA of interscapular BAT (A) and skeletal muscle (tibialis anterior) (B) hybridized to UCP1, UCP2, or UCP3 cDNA. UCP mRNA levels were normalized to β-actin mRNA levels, and the data are expressed as percentage of WT levels. At least five tissues were analyzed per genotype. Values depict mean ± SEM (*, $P<0.05$).

trols (Fig. 8). Basal glucose transport was lower in PTP-1B$^{-/-}$ adipocytes (Fig. 8A). This likely reflects the fact that PTP-1B$^{-/-}$ adipocytes are smaller than those of control mice, since previous work showed that basal transport is proportional to adipocyte size (23). The maximal glucose transport rates (54.3 ± 0.74 amol min^{-1} cell^{-1} for PTP-1B$^{-/-}$ versus 49.0 ± 5.87 amol min^{-1} for PTP-1B$^{+/+}$; $P = 0.44$) were not significantly different in PTP-1B$^{-/-}$ and WT adipocytes. Likewise, the 50% effective concentrations for glucose transport were similar (1.10 ± 0.294 nM for PTP-1B$^{-/-}$ versus 2.22 ± 1.98 for PTP-1B$^{+/+}$; $P = 0.62$) (Fig. 8B). Taken together, these results indicate that the enhanced insulin sensitivity in PTP-1B-deficient mice is tissue specific.

DISCUSSION

This work reports the generation and characterization of PTP-1B-deficient (Ex1$^{-/-}$) mice. These mice are leaner than WT mice and have dramatically decreased white adipose stores. Moreover, their energy expenditure is increased substantially, and thus they are less metabolically efficient, accounting for their resistance to diet-induced obesity. PTP-1B-deficient mice display enhanced insulin sensitivity in hyperinsulinemic-euglycemic clamp studies, as manifested by significant increases in rates of whole-body glucose disposal, glycolysis, and nonoxidative glucose metabolism. Interestingly, insulin sensitivity in PTP-1B$^{-/-}$ mice is elevated specifically in skeletal muscle, not in white adipose tissue. Our work indicates that PTP-1B plays a crucial role in regulating energy balance, the accumulation of body fat stores, and insulin sensitivity in some, but not all, tissues.

Elchebly et al. (28) reported that PTP-1B Ex5/6$^{-/-}$ mice are resistant to body weight gain on a high-fat diet, but the physiological basis for their observations was unclear. Here, we show that the leanness of PTP-1B-deficient mice results from increases in both BMR and the non-BMR-related component of energy expenditure. Removal of PTP-1B results in significant changes in body composition relative to WT mice, as evidenced by a marked reduction in the mass of white fat depots and body lipid content and a smaller reduction in fat free dry mass (Fig. 3; Tables 1 and 2). This reflects a 61% decrease in adipocyte volume (micrograms of lipid per cell), without alteration of fat cell number. Our results identify PTP-1B as an important new regulator of energy expenditure and body composition.

Absence of PTP-1B in mice results in increased insulin sensitivity in skeletal muscle, leading to enhanced glucose tolerance and an 80% increase in insulin-stimulated whole-body glucose disposal. The enhanced insulin sensitivity in skeletal muscle of PTP-1B Ex1$^{-/-}$ mice correlates with abnormal (hyper- and/or sustained) tyrosyl phosphorylation of IR/IRS-1 in this tissue (28) and thus with previous suggestions that PTP-1B is a physiologically relevant IR phosphatase (see the introduction). The reason why PTP-1B apparently is a less important regulator of insulin-stimulated glucose uptake in adipose tissue is unclear. Conceivably, other PTPs play a more important role in adipose tissue. Alternatively, IR trafficking in adipocytes could differ from that in skeletal muscle. PTP-1B is located on intracellular membranes, and thus its ability to access tyrosyl phosphorylated IRs may vary between cell types.

There are some differences between our findings and those published previously (28). First, we observed a significantly lower body weight for both PTP-1B Ex1$^{-/-}$ and heterozygotic Ex1$^{+/-}$ mice (compared to WT mice) on a chow diet, whereas Elchebly et al. (28) reported no significant difference in weight gain between WT, heterozygotic, and homozygotic chow-fed mice. The most likely explanation for this discrepancy is that their chow diet contained nearly half as much fat as ours (M. L. Tremblay, personal communication). Second, in our study, chow-fed female PTP-1B Ex1$^{-/-}$ mice were less susceptible than male mice to the effects of PTP-1B deficiency. In contrast, Elchebly et al. (28) did not report any gender-specific differences. These findings might also be attributed to the different

TABLE 3. Metabolic characteristics of WT, PTP-1B$^{+/-}$, and PTP-1B$^{-/-}$ mice fed either a chow or a high-fat diet[a]

Parameter	Chow diet			High-fat diet		
	WT	PTP-1B$^{+/-}$	PTP-1B$^{-/-}$	WT	PTP-1B$^{+/-}$	PTP-1B$^{-/-}$
Fed, serum leptin (ng ml^{-1})	7.86 ± 1.16^{a}	5.59 ± 0.41^{a,b}	5.02 ± 0.42^{b}	13.37 ± 2.57^{a}	9.36 ± 2.32^{b}	5.24 ± 1.15^{c}
Serum FFA (mM)						
Fed	0.90 ± 0.08^{a}	0.89 ± 0.05^{a}	0.88 ± 0.04^{a}	0.54 ± 0.05^{a}	0.53 ± 0.07^{a}	0.63 ± 0.06^{a}
Fasted	1.77 ± 0.14^{a}	ND	1.46 ± 0.08^{a}	1.31 ± 0.07^{a}	1.55 ± 0.07^{a}	1.42 ± 0.08^{a}
Blood glucose (mg dl^{-1})						
Fed	133 ± 4.73^{a}	124 ± 4.35^{a}	114 ± 2.54^{b}	132 ± 4.62^{a}	126 ± 5.60^{a,b}	115 ± 3.50^{b}
Fasted	67.7 ± 2.74^{a}	62.2 ± 2.58^{a}	57.5 ± 2.67^{b}	79.9 ± 3.83^{a}	77.3 ± 7.68^{a,b}	66.6 ± 3.87^{b}
Serum insulin (ng ml^{-1})						
Fed	1.89 ± 0.28^{a}	1.21 ± 0.09^{a,b}	0.81 ± 0.10^{b}	1.57 ± 0.22^{a}	1.75 ± 0.18^{a}	0.59 ± 0.09^{b}
Fasted	0.36 ± 0.07^{a}	0.25 ± 0.03^{a}	0.27 ± 0.03^{a}	0.50 ± 0.05^{a}	0.53 ± 0.11^{a,b}	0.35 ± 0.05^{b}

[a] Male PTP-1B$^{-/-}$, PTP-1B$^{+/-}$, or WT mice were fed a chow or high-fat diet ad libitum. Serum was collected from fed or fasted mice between 8 and 10 weeks of age, and the indicated metabolic parameters were measured. Values are expressed as the mean ± SEM of measurements obtained for 6 to 10 animals per group. ND, not determined. Within a particular diet, values in the same row not sharing a superscript letter are significantly different ($P < 0.05$).

Downloaded from http://mcb.asm.org/ on June 25, 2019 by guest

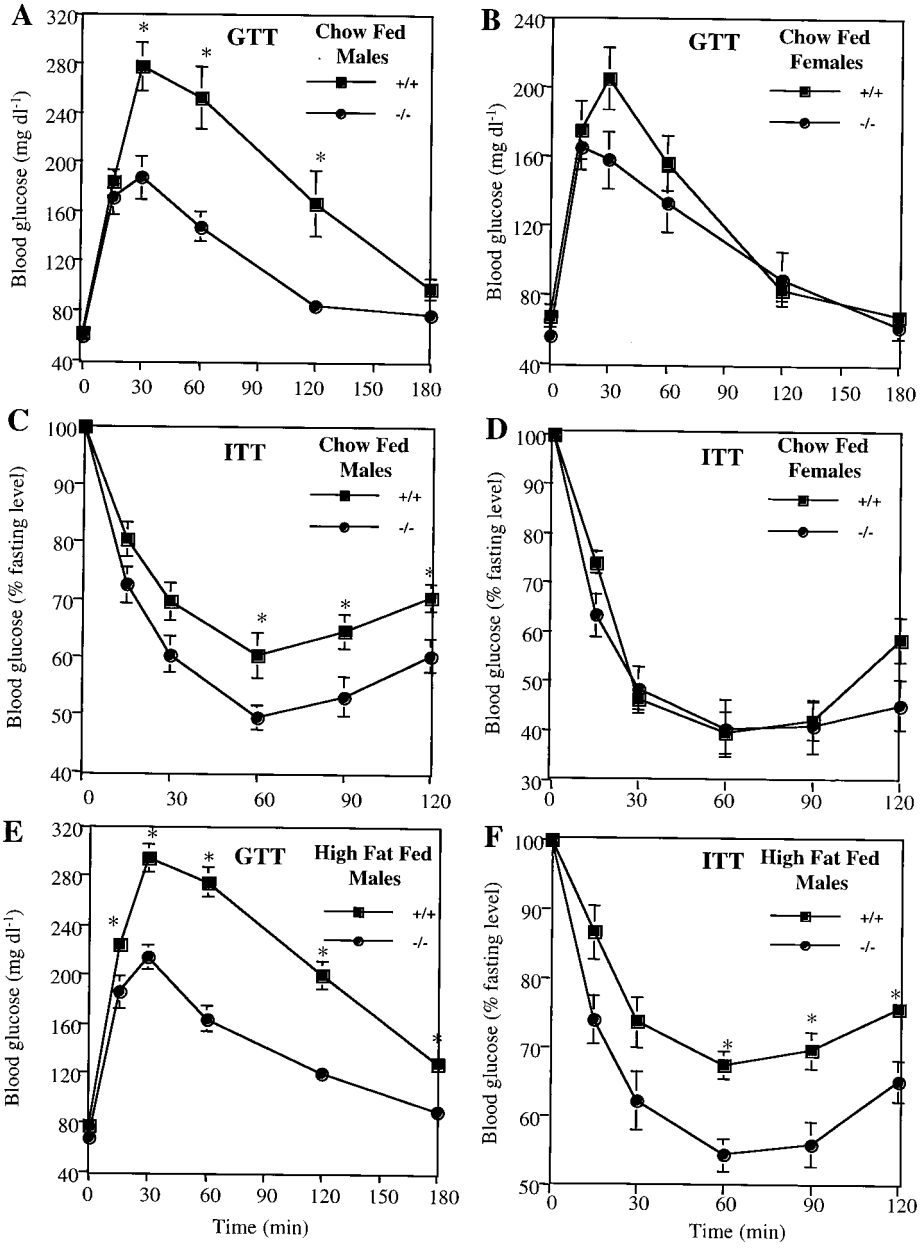

FIG. 6. GTT and ITT on PTP-1B$^{-/-}$ (−/−) and WT (+/+) mice. (A) GTT on 12-week-old chow-fed males; (B) GTT on 12-week-old chow-fed females; (C) ITT on 14-week-old chow-fed males; (D) ITT on 14-week-old chow-fed females; (E and F) GTT (E) and ITT (F) on 16-week-old high-fat-fed males. For ITTs, blood glucose values are expressed as a percentage of initial concentration. Experimental groups consisted of 9 to 10 mice, and tests were performed a minimum of three times with similar outcomes. Values depict mean ± SEM. An asterisk indicates differences between PTP-1B$^{-/-}$ and WT groups where $P < 0.05$.

chow diets or to differences in genetic background, since our mice were analyzed on the C57BL6/J × 129/SvJ background whereas mice in their study were C57BL6/J × BALB/c.

Interestingly, on a chow diet, body weights (Fig. 2) and serum insulin levels (fasted and fed) (Table 3) of our heterozygotic PTP-1B Ex1$^{+/-}$ animals were similar to those of Ex1$^{-/-}$ mice, whereas on the high-fat diet, Ex1$^{+/-}$ mouse weights and serum insulin levels were more similar to those of WT controls. This suggests that on the high-fat, but not chow, diet, one copy of the PTP-1B gene is sufficient to mediate its effects on energy expenditure and insulin action. Conceivably, PTP-1B expression might be regulated by diet. Indeed, we have found recently that the expression of PTP-1B mRNA is increased significantly in skeletal muscle (+70%, $P = 0.016$), but not in white adipose tissue (+1%, $P = 0.99$), of mice fed a high-fat diet (O. Boss and L. D. Klaman, unpublished data). These results may explain, at least in part, the influence of the chow and high-fat diets on the body weight and insulin sensitivity of the heterozygotic Ex1$^{+/-}$ mice.

The most interesting and important question raised by this study concerns the relationship between the enhanced insulin sensitivity and the increased energy expenditure in the PTP-1B-deficient mice. There are three general classes of explanation. First, since insulin sensitivity is usually increased in lean individuals (25), the increased energy expenditure in PTP-1B-deficient mice might result in decreased adipose stores, which

Downloaded from http://mcb.asm.org/ on June 25, 2019 by guest

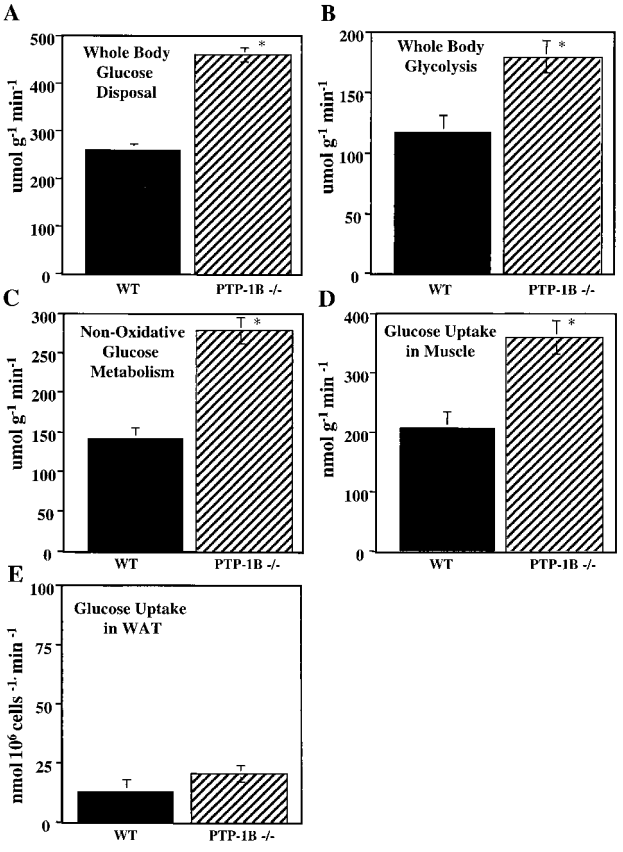

FIG. 7. Hyperinsulinemic-euglycemic clamp studies in conscious PTP-1B$^{-/-}$ and WT mice. Whole-body glucose disposal rate (A), whole-body glycolysis rate (B), whole-body nonoxidative glucose metabolic rate (C) glucose uptake in skeletal muscle (gastocnemius) (D), and glucose uptake in white adipose tissue (WAT; epididymal fat pad; E) were determined for fasted, 16-week-old male mice. Results are the mean ± SEM for five animals per genotype (*, $P < 0.05$).

in turn would lead to enhanced insulin sensitivity. In this model, the primary role of PTP-1B would be to control a pathway(s) that regulates energy expenditure, with any effect on insulin signaling being secondary. We do not favor this explanation for two reasons. Although PTP-1B Ex1$^{-/-}$ mice are both insulin sensitive and lean under all conditions tested, Elchebly et al. (28) reported significantly enhanced insulin sensitivity in PTP-1B Ex5/6$^{-/-}$ and Ex5/6$^{+/-}$ mice under conditions (their chow diet) in which they detected no alteration in body weight. Moreover, several studies suggest that PTP-1B directly dephosphorylates the IR (see the introduction) and the IR is hyperphosphorylated in PTP-1B-deficient mice (28).

A second possibility is that the increased insulin sensitivity in the skeletal muscle of PTP-1B$^{-/-}$ mice leads to a higher metabolic rate, resulting in decreased white adipose mass in these mice. Precisely how increased insulin sensitivity might lead to decreased metabolic efficiency in PTP-1B$^{-/-}$ mice remains to be determined, but increased mitochondrial proton leaks through UCPs or other mechanisms and/or increased activity of futile cycles could mediate this enhanced energy dissipation (50). Notably, our data show similar mRNA expression of UCPs in skeletal muscle of WT and PTP-1B$^{-/-}$ mice (Fig. 5). This suggests that skeletal muscle UCPs are unlikely mediators of the increased metabolic rate in PTP-1B$^{-/-}$ mice. However, we cannot exclude the possibility that UCP activity might somehow be increased. Insulin may also influence metabolic rate by acting on the central nervous system. For example, insulin stimulation of hypothalamic neurons increases sympathetic stimulation of BAT, leading to an increase in energy expenditure (57, 66). The major mechanism by which this occurs in rodents is by increasing brown fat mass and UCP expression (64). UCP mRNA levels in BAT of PTP-1B$^{-/-}$ mice were similar overall to those of WT mice. There was a small increase in UCP3 mRNA expression in BAT (Fig. 5); the physiological significance of this increase is questionable. Moreover, there was no increase in BAT mass in PTP-1B$^{-/-}$ animals, suggesting that PTP-1B is unlikely to regulate the sympathetic activity in BAT. In addition, insulin action in the central nervous system results in decreased food intake (55), contrasting with the slightly increased food intake that we observe in our PTP-1B Ex1$^{-/-}$ mice.

Finally, the increased energy expenditure and increased insulin sensitivity could reflect regulation of distinct signaling pathways by PTP-1B. In this model, the increased insulin sensitivity observed in the absence of PTP-1B would result from failure to appropriately dephosphorylate the IR (and possi-

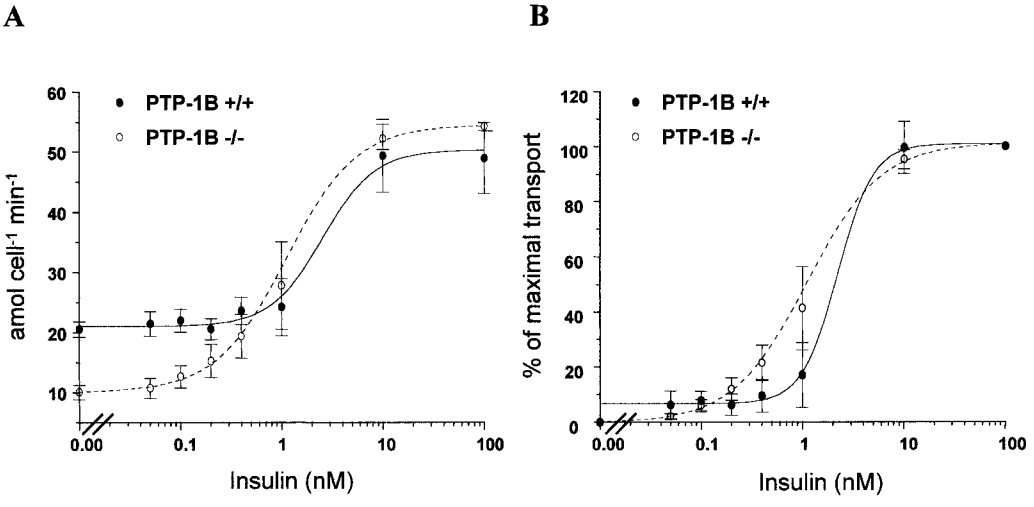

FIG. 8. Insulin dose-response curves for glucose transport into isolated adipocytes from WT and PTP-1B$^{-/-}$ mice. Adipocytes were isolated and incubated with various concentrations of insulin as described in Materials and Methods. Expression of data as percentage of maximal transport (B) corrects for differences in basal rates of transport. Values for both panels are means ± SEM for four WT and four PTP-1B$^{-/-}$ male mice that were 12 weeks of age.

Downloaded from http://mcb.asm.org/ on June 25, 2019 by guest

bly IRS proteins), whereas the enhanced energy expenditure would reflect altered regulation of as yet unidentified targets that regulate metabolic rate. Our work, together with that of Elchebly et al. (28), identifies PTP-1B as a promising new target for intervention in obesity and insulin resistance.

ACKNOWLEDGMENTS

We thank Bruce M. Spiegelman, Bradford B. Lowell, Jeffrey S. Flier, and Thomas McGarry for comments on the manuscript, William G. Tsiaras for technical help, and Lena Du and Joel Lawitts for blastocyst injections.

This work was supported by grants from the Human Frontier Science Program (LT0020/1999 to O.B.) and the National Institutes of Health (NRSA-AI09815 to L.D.K.; NRSA-DK09903 to J.M.Z.; P01 DK 56116, P30-DK46200, and RO1-DK-43051 to B.B.K.; PO1-DK50654 and RO1-CA49152 to B.G.N.; and P30-DK45735 and RO1-DK40936 to G.I.S.). G.I.S. is an investigator and J.K.K. is a research associate of the Howard Hughes Medical Institute. O.D.P. was supported by an ADA mentor-based fellowship (to B.B.K.).

REFERENCES

1. **Ahmad, F., J. L. Azevedo, R. Cortright, G. L. Dohm, and B. J. Goldstein.** 1997. Alterations in skeletal muscle protein-tyrosine phosphatase activity and expression in insulin-resistant human obesity and diabetes. J. Clin. Investig. **100:**449–458.
2. **Ahmad, F., R. V. Considine, T. L. Bauer, J. P. Ohannesian, C. C. Marco, and B. J. Goldstein.** 1997. Improved sensitivity to insulin in obese subjects following weight loss is accompanied by reduced protein-tyrosine phosphatases in adipose tissue. Metabolism **46:**1140–1145.
3. **Ahmad, F., R. V. Considine, and B. J. Goldstein.** 1995. Increased abundance of the receptor-type protein-tyrosine phosphatase LAR accounts for the elevated insulin receptor dephosphorylating activity in adipose tissue of obese human subjects. J. Clin. Investig. **95:**2806–2812.
4. **Ahmad, F., and B. J. Goldstein.** 1995. Alterations in specific protein-tyrosine phosphatases accompany insulin resistance of streptozotocin diabetes. Am. J. Physiol. **268:**E932–E940.
5. **Ahmad, F., and B. J. Goldstein.** 1995. Purification, identification and subcellular distribution of three predominant protein-tyrosine phosphatase enzymes in skeletal muscle tissue. Biochim. Biophys. Acta **1248:**57–69.
6. **Ahmad, F., and B. J. Goldstein.** 1995. Increased abundance of specific skeletal muscle protein-tyrosine phosphatases in a genetic model of insulin-resistant obesity and diabetes mellitus. Metabolism **44:**1175–1184.
7. **Ahmad, F., P. M. Li, J. Meyerovitch, and B. J. Goldstein.** 1995. Osmotic loading of neutralizing antibodies demonstrates a role for protein-tyrosine phosphatase 1B in negative regulation of the insulin action pathway. J. Biol. Chem. **270:**20503–20508.
8. **Arregui, C. O., J. Balsamo, and J. Lilien.** 1998. Impaired integrin-mediated adhesion and signaling in fibroblasts expressing a dominant-negative mutant PTP1B. J. Cell Biol. **143:**861–873. (Erratum, 143:1761, 1998.)
9. **Astrup, A.** 1999. Macronutrient balances and obesity: the role of diet and physical activity. Public Health Nutr. **2:**341–347.
10. **Balsamo, J., C. Arregui, T. Leung, and J. Lilien.** 1998. The nonreceptor protein tyrosine phosphatase PTP1B binds to the cytoplasmic domain of N-cadherin and regulates the cadherin-actin linkage. J. Cell Biol. **143:**523–532.
11. **Baskin, D. G., T. M. Hahn, and M. W. Schwartz.** 1999. Leptin sensitive neurons in the hypothalamus. Horm. Metab. Res. **31:**345–350.
12. **Begum, N., K. E. Sussman, and B. Draznin.** 1991. Differential effects of diabetes on adipocyte and liver phosphotyrosine and phosphoserine phosphatase activities. Diabetes **40:**1620–1629.
13. **Bleyle, L. A., Y. Peng, C. Ellis, and R. A. Mooney.** 1999. Dissociation of PTPase levels from their modulation of insulin receptor signal transduction. Cell Signal **11:**719–725.
14. **Boss, O., S. Samec, A. Paoloni-Giacobino, C. Rossier, A. Dulloo, J. Seydoux, P. Muzzin, and J. P. Giacobino.** 1997. Uncoupling protein-3: a new member of the mitochondrial carrier family with tissue-specific expression. FEBS Lett. **408:**39–42.
15. **Boss, O., E. Bachman, A. Vidal-Puig, C. Y. Zhang, O. Peroni, and B. B. Lowell.** 1999. Role of the beta(3)-adrenergic receptor and/or a putative beta(4)-adrenergic receptor on the expression of uncoupling proteins and peroxisome proliferator-activated receptor-gamma coactivator-1. Biochem. Biophys. Res. Commun. **261:**870–876.
16. **Boss, O., T. Hagen, and B. B. Lowell.** 2000. Uncoupling proteins 2 and 3: potential regulators of mitochondrial energy metabolism. Diabetes **49:**143–156.
17. **Boylan, J. M., D. L. Brautigan, J. Madden, T. Raven, L. Ellis, and P. A. Gruppuso.** 1992. Differential regulation of multiple hepatic protein tyrosine phosphatases in alloxan diabetic rats. J. Clin. Investig. **90:**174–179.
18. **Bray, M. S.** 2000. Genomics, genes, and environmental interaction: the role of exercise. J. Appl. Physiol. **88:**788–792.
19. **Byon, J. C., A. B. Kusari, and J. Kusari.** 1998. Protein-tyrosine phosphatase-1B acts as a negative regulator of insulin signal transduction. Mol. Cell. Biochem. **182:**101–108.
20. **Cheung, A., J. Kusari, D. Jansen, D. Bandyopadhyay, A. Kusari, and M. Bryer-Ash.** 1999. Marked impairment of protein tyrosine phosphatase 1B activity in adipose tissue of obese subjects with and without type 2 diabetes mellitus. J. Lab. Clin. Med. **134:**115–123.
21. **Cousin, B., S. Cinti, M. Morroni, S. Raimbault, D. Ricquier, L. Penicaud, and L. Casteilla.** 1992. Occurrence of brown adipocytes in rate white adipose tissue: molecular and morphological characterization. J. Cell Sci. **103:**931–942.
22. **Cushman, S. W., and L. B. Salans.** 1978. Determinations of adipose cell size and number in suspensions of isolated rat and human adipose cells. J. Lipid Res. **19:**269–273.
23. **Czech, M. P.** 1976. Cellular basis of insulin insensitivity in large rat adipocytes. J. Clin. Investig. **57:**1523–1532.
24. **Czech, M. P., and S. Corvera.** 1999. Signaling mechanisms that regulate glucose transport. J. Biol. Chem. **274:**1865–1868.
25. **DeFronzo, R. A.** 1997. Pathogenesis of type 2 diabetes: metabolic and molecular implications for identifying diabetes genes. Diabetes Rev. **5:**177–269.
26. **Di Guglielmo, G. M., P. G. Drake, P. C. Baass, F. Authier, B. I. Posner, and J. J. Bergeron.** 1998. Insulin receptor internalization and signalling. Mol. Cell. Biochem. **182:**59–63.
27. **Echwald, S. M.** 1999. Genetics of human obesity: lessons from mouse models and candidate genes. J. Intern. Med. **245:**653–666.
28. **Elchebly, M., P. Payette, E. Michaliszyn, W. Cromlish, S. Collins, A. L. Loy, D. Normandin, A. Cheng, J. Himms-Hagen, C. C. Chan, C. Ramachandran, M. J. Gresser, M. L. Tremblay, and B. P. Kennedy.** 1999. Increased insulin sensitivity and obesity resistance in mice lacking the protein tyrosine phosphatase-1B gene. Science **283:**1544–1548.
29. **Elmquist, J. K., E. Maratos-Flier, C. B. Saper, and J. S. Flier.** 1998. Unraveling the central nervous system pathways underlying responses to leptin. Nat. Neurosci. **1:**445–450.
30. **Faure, R., G. Baquiran, J. J. Bergeron, and B. I. Posner.** 1992. The dephosphorylation of insulin and epidermal growth factor receptors. Role of endosome-associated phosphotyrosine phosphatase(s). J. Biol. Chem. **267:**11215–11221.
31. **Fleury, C., M. Neverova, S. Collins, S. Raimbault, O. Champigny, C. Levi-Meyrueis, F. Bouillaud, M. F. Seldin, R. S. Surwit, D. Ricquier, and C. H. Warden.** 1997. Uncoupling protein-2: a novel gene linked to obesity and hyperinsulinemia. Nat. Genet. **15:**269–272.
32. **Flint, A. J., M. F. Gebbink, B. R. Franza, Jr., D. E. Hill, and N. K. Tonks.** 1993. Multi-site phosphorylation of the protein tyrosine phosphatase, PTP1B: identification of cell cycle regulated and phorbol ester stimulated sites of phosphorylation. EMBO J. **12:**1937–1946.
33. **Flint, A. J., T. Tiganis, D. Barford, and N. K. Tonks.** 1997. Development of "substrate-trapping" mutants to identify physiological substrates of protein tyrosine phosphatases. Proc. Natl. Acad. Sci. USA **94:**1680–1685.
34. **Foreyt, J. P., and W. S. Poston II.** 1999. The challenge of diet, exercise and lifestyle modification in the management of the obese diabetic patient. Int. J. Obes. Relat. Metab. Disord. **23**(Suppl. 7)**:**S5–S11.
35. **Frangioni, J. V., P. H. Beahm, V. Shifrin, C. A. Jost, and B. G. Neel.** 1992. The nontransmembrane tyrosine phosphatase PTP-1B localizes to the endoplasmic reticulum via its 35 amino acid C-terminal sequence. Cell **68:**545–560.
36. **Goldstein, B. J., F. Ahmad, W. Ding, P. M. Li, and W. R. Zhang.** 1998. Regulation of the insulin signalling pathway by cellular protein-tyrosine phosphatases. Mol. Cell. Biochem. **182:**91–99.
37. **Grimm, J. J.** 1999. Interaction of physical activity and diet: implications for insulin-glucose dynamics. Public Health Nutr. **2:**363–368.
38. **Guerra, C., R. A. Koza, H. Yamashita, K. Walsh, and L. P. Kozak.** 1998. Emergence of brown adipocytes in white fat in mice is under genetic control. Effects on body weight and adiposity. J. Clin. Investig. **102:**412–420.
39. **Hashimoto, N., E. P. Feener, W. R. Zhang, and B. J. Goldstein.** 1992. Insulin receptor protein-tyrosine phosphatases. Leukocyte common antigen-related phosphatase rapidly deactivates the insulin receptor kinase by preferential dephosphorylation of the receptor regulatory domain. J. Biol. Chem. **267:**13811–13814.
40. **Hauguel-de Mouzon, S., P. Peraldi, F. Alengrin, and E. Van Obberghen.** 1993. Alteration of phosphotyrosine phosphatase activity in tissues from diabetic and pregnant rats. Endocrinology **132:**67–74.
41. **Himms-Hagen, J.** 1989. Brown adipose tissue thermogenesis and obesity. Prog. Lipid Res. **28:**67–115.
42. **Kahn, C. R.** 1994. Banting Lecture. Insulin action, diabetogenes, and the cause of type II diabetes. Diabetes **43:**1066–1084.
43. **Kao, A. W., S. B. Waters, S. Okada, and J. E. Pessin.** 1997. Insulin stimulates the phosphorylation of the 66- and 52-kilodalton Shc isoforms by distinct pathways. Endocrinology **138:**2474–2480.
44. **Kenner, K. A., D. E. Hill, J. M. Olefsky, and J. Kusari.** 1993. Regulation of

Downloaded from http://mcb.asm.org/ on June 25, 2019 by guest

protein tyrosine phosphatases by insulin and insulin-like growth factor I. J. Biol. Chem. **268:**25455–25462.
45. **Kenner, K. A., E. Anyanwu, J. M. Olefsky, and J. Kusari.** 1996. Protein-tyrosine phosphatase 1B is a negative regulator of insulin- and insulin-like growth factor-I-stimulated signaling. J. Biol. Chem. **271:**19810–19819.
46. **Kuhne, M. R., T. Pawson, G. E. Lienhard, and G. S. Feng.** 1993. The insulin receptor substrate 1 associates with the SH2-containing phosphotyrosine phosphatase Syp. J. Biol. Chem. **268:**11479–11481.
47. **Kusari, J., K. A. Kenner, K. I. Suh, D. E. Hill, and R. R. Henry.** 1994. Skeletal muscle protein tyrosine phosphatase activity and tyrosine phosphatase 1B protein content are associated with insulin action and resistance. J. Clin. Investig. **93:**1156–1162.
48. **Liu, F., D. E. Hill, and J. Chernoff.** 1996. Direct binding of the proline-rich region of protein tyrosine phosphatase 1B to the Src homology 3 domain of p130(Cas). J. Biol. Chem. **271:**31290–31295.
49. **Liu, F., M. A. Sells, and J. Chernoff.** 1998. Protein tyrosine phosphatase 1B negatively regulates integrin signaling. Curr. Biol. **8:**173–176.
50. **Lowell, B. B., and B. M. Spiegelman.** 2000. Towards a molecular understanding of adaptive thermogenesis. Nature **404:**652–660.
51. **Maegawa, H., M. Hasegawa, S. Sugai, T. Obata, S. Ugi, K. Morino, K. Egawa, T. Fujita, T. Sakamoto, Y. Nishio, H. Kojima, M. Haneda, H. Yasuda, R. Kikkawa, and A. Kashiwagi.** 1999. Expression of a dominant negative SHP-2 in transgenic mice induces insulin resistance. J. Biol. Chem. **274:** 30236–30243.
52. **McGuire, M. C., R. M. Fields, B. L. Nyomba, I. Raz, C. Bogardus, N. K. Tonks, and J. Sommercorn.** 1991. Abnormal regulation of protein tyrosine phosphatase activities in skeletal muscle of insulin-resistant humans. Diabetes **40:**939–942.
53. **Myers, M. G., Jr., R. Mendez, P. Shi, J. H. Pierce, R. Rhoads, and M. F. White.** 1998. The COOH-terminal tyrosine phosphorylation sites on IRS-1 bind SHP-2 and negatively regulate insulin signaling. J. Biol. Chem. **273:** 26908–26914.
53a. **National Institutes of Health.** 1985. Guide for the care and use of laboratory animals, rev. ed. Department of Health and Human Services publication no. (NIH) 85-23. National Institutes of Health, Bethesda, Md.
54. **Olefsky, J. M.** 1999. Insulin-stimulated glucose transport minireview series. J. Biol. Chem. **274:**1863.
55. **Porte, D., Jr., R. J. Seeley, S. C. Woods, D. G. Baskin, D. P. Figlewicz, and M. W. Schwartz.** 1998. Obesity, diabetes and the central nervous system. Diabetologia **41:**863–881.
56. **Ren, J. M., B. A. Marshall, M. M. Mueckler, M. McCaleb, J. M. Amatruda, and G. I. Shulman.** 1995. Overexpression of Glut4 protein in muscle increases basal and insulin-stimulated whole body glucose disposal in conscious mice. J. Clin. Investig. **95:**429–432.
57. **Ricquier, D., G. Mory, F. Bouillaud, M. Combes-George, and J. Thibault.** 1985. Factors controlling brown adipose tissue development. Reprod. Nutr. Dev. **25:**175–181.
58. **Ricquier, D., and F. Bouillaud.** 2000. The uncoupling protein homologues: UCP1, UCP2, UCP3, StUCP and AtUCP. Biochem. J. **345:**161–179.
59. **Rothwell, N. J., and M. J. Stock.** 1979. A role for brown adipose tissue in diet-induced thermogenesis. Nature **281:**31–35.
60. **Salmon, D. M., and J. P. Flatt.** 1985. Effect of dietary fat content on the incidence of obesity among ad libitum fed mice. Int. J. Obes. **9:**443–449.
61. **Schievella, A. R., L. A. Paige, K. A. Johnson, D. E. Hill, and R. L. Erikson.** 1993. Protein tyrosine phosphatase 1B undergoes mitosis-specific phosphorylation on serine. Cell Growth Differ. **4:**239–246.
62. **Seely, B. L., P. A. Staubs, D. R. Reichart, P. Berhanu, K. L. Milarski, A. R. Saltiel, J. Kusari, and J. M. Olefsky.** 1996. Protein tyrosine phosphatase 1B interacts with the activated insulin receptor. Diabetes **45:**1379–1385.
63. **Shifrin, V. I., R. J. Davis, and B. G. Neel.** 1997. Phosphorylation of protein-tyrosine phosphatase PTP-1B on identical sites suggests activation of a common signaling pathway during mitosis and stress response in mammalian cells. J. Biol. Chem. **272:**2957–2962.
64. **Silva, J. E., and R. Rabelo.** 1997. Regulation of the uncoupling protein gene expression. Eur. J. Endocrinol. **136:**251–264.
65. **Stock, M. J., and N. J. Rothwell.** 1985. Factors influencing brown fat and the capacity for diet-induced thermogenesis. Int. J. Obes. **9**(Suppl. 2)**:**9–15.
66. **Strack, A. M., C. J. Horsley, R. J. Sebastian, S. F. Akana, and M. F. Dallman.** 1995. Glucocorticoids and insulin: complex interaction on brown adipose tissue. Am. J. Physiol. **268:**R1209–R1216.
67. **Tozzo, E., L. Gnudi, and B. B. Kahn.** 1997. Amelioration of insulin resistance in streptozotocin diabetic mice by transgenic overexpression of GLUT4 driven by an adipose-specific promoter. Endocrinology **138:**1604–1611.
68. **Ugi, S., H. Maegawa, A. Kashiwagi, M. Adachi, J. M. Olefsky, and R. Kikkawa.** 1996. Expression of dominant negative mutant SHPTP2 attenuates phosphatidylinositol 3′-kinase activity via modulation of phosphorylation of insulin receptor substrate-1. J. Biol. Chem. **271:**12595–12602.
69. **White, M. F.** 1998. The IRS-signalling system: a network of docking proteins that mediate insulin action. Mol. Cell. Biochem. **182:**3–11.
70. **Williams, G.** 1999. Obesity and type 2 diabetes: a conflict of interests? Int. J. Obes. Relat. Metab. Disord. **23**(Suppl. 7)**:**S2–S4.
71. **Woodford-Thomas, T. A., J. D. Rhodes, and J. E. Dixon.** 1992. Expression of a protein tyrosine phosphatase in normal and v-src-transformed mouse 3T3 fibroblasts. J. Cell Biol. **117:**401–414.
72. **Worm, D., J. Vinten, P. Staehr, J. E. Henriksen, A. Handberg, and H. Beck-Nielsen.** 1996. Altered basal and insulin-stimulated phosphotyrosine phosphatase (PTPase) activity in skeletal muscle from NIDDM patients compared with control subjects. Diabetologia **39:**1208–1214.
73. **Youn, J. H., J. K. Kim, and G. M. Steil.** 1995. Assessment of extracellular glucose distribution and glucose transport activity in conscious rats. Am. J. Physiol. **268:**E712–E7121.
74. **Zhang, Y., R. Proenca, M. Maffei, M. Barone, L. Leopold, and J. M. Friedman.** 1994. Positional cloning of the mouse obese gene and its human homologue. Nature **372:**425–432. (Erratum, 374:479, 1995.)

Downloaded from http://mcb.asm.org/ on June 25, 2019 by guest